

Conf-9209100--22  
Nov 1 1992

## Computer Modeling of Fluidized-Beds

J.X. Bouillard, R.W. Lyczkowski and J. Ding  
Energy Systems Division  
Argonne National Laboratory  
Argonne, Illinois, USA

ANL/CP--77469

DE93 003002

Authored  
document  
ENG-38.  
contains a  
tabular  
table  
this  
for

### ABSTRACT

*Bubbling fluidized-bed combustors are being built as a means of burning high-sulfur coals in an environmentally acceptable manner. Although this technology has reached a commercial status, understanding of solids motion and its effect on erosion of heat exchanger tubes immersed in fluidized beds remains inadequate. To understand the mechanics of solids motion in fluidized beds with internal heat exchangers, a two-dimensional fluidized bed is simulated using hydrodynamic models. Predicted instantaneous and time-averaged porosities at different locations in the bed are compared with experimentally measured values. Power spectral analyses of both computed and experimental transient porosities are made to validate the presently used hydrodynamic model of fluidization. This study further extends the validation of such models used in earlier studies to compare experimental and predicted bubble sizes.*

### INTRODUCTION

To predict bubble and solids motion in fluidized-beds is important in understanding the stability and scale-up of fossil fuel gasifiers and combustors. These motions profoundly affect the exchange of heat and mass between the phases. Much experimental work in gas-solid [1] and gas-liquid-solid [2] fluidized-beds has been carried out over the last 30 years attempting to understand bubble formation, frequency, size and velocity and how they affect the mechanisms of gasification and combustion. Solids motion studies are less common because of the experimental difficulties involved [3].

Over this same period of time, many models have been proposed for studying these phenomena in fluidized-bed combustors (FBCS) - about 30 according to three recent reviews [1,4,5]. The one-dimensional models, which predominate, include gas composition and pollutant formation in one dimension and rely heavily on simplifying assumptions to avoid the treatment of complex fluid motion.

The hydrodynamic approach to fluidization which started with Davidson in 1961 [6] serves as the basis of the three extant two-dimensional fluidized-bed codes CHEMFLUB, FLAG and IIT, the last of which we also call FLUFLIX. The capabilities of these codes were reviewed by Smoot [5] and Gidaspow [7]. The progress made in the last 6 years modeling small-scale highly instrumental "two-dimensional" fluidized-beds at the Illinois Institute of Technology (IIT) using the FLUFLIX computer code has served to validate the hydrodynamic model in a great part [8-13] and has been reviewed recently by Gidaspow [7].

Almost non-existent is the understanding of how bubbles interact with solids surfaces within fluidized-beds. These surfaces may take the form of instrument probes to detect the bubbles themselves [14] and, in the case of fluidized-bed combustors, heat exchanger tubes and baffles placed either in the bed or in the free-board or both [15,16]. The purpose of this study is to investigate the interaction between bubbles and solid surfaces both theoretically and experimentally by comparing computed and experimental transient porosities near solid surfaces.

A fluidized-bed is inherently oscillatory with no true steady-state ever achieved. Thus, our hydrodynamic computer modeling is time-dependent and two-dimensional.

**MASTER**

## HYDRODYNAMIC MODEL

Hydrodynamic models of fluidization use the principles of conservation of mass, momentum and energy. Table I shows the continuity and the separate phase momentum equations for transient isothermal multiphase flow which form the basis of the two-dimensional Cartesian and axisymmetric cylindrical FLUFIX computer program. There are six nonlinear coupled partial differential equations in two dimensions for the six dependent variables to be computed: the void fraction,  $\epsilon$ , the pressure,  $P$ , the gas velocity components  $U_g$ ,  $V_g$ , and the solids velocity components  $U_s$  and  $V_s$ , in the  $x$  and  $y$  directions, respectively. The equations are written in a form similar to that used in the K-FIX computer code [17] from which FLUFIX has been developed.

Table I Hydrodynamic Model

### Continuity

$$\frac{\partial}{\partial t}(\epsilon_k \rho_k) + \nabla \cdot (\epsilon_k \rho_k \vec{v}_k) = 0 \quad (1)$$

### Momentum

$$\frac{\partial}{\partial t}(\epsilon_k \rho_k \vec{v}_k) + \nabla \cdot (\epsilon_k \rho_k \vec{v}_k \vec{v}_k) = \nabla \cdot \bar{\sigma}_{ke} + \epsilon_k \rho_k \vec{g} + \sum_{i=1}^n \bar{\beta}_{ik} \cdot (\vec{v}_i - \vec{v}_k) \quad (2)$$

Acceleration                      Stress      Gravity                      Interphases Drag

with

$$\nabla \cdot \bar{\sigma}_{ke} = \begin{cases} -\epsilon_k \nabla \cdot (p \bar{I}) + \nabla \cdot (\epsilon_k \bar{\tau}_{kv}) - \delta_{kxi} \nabla \cdot \bar{\tau}_{kc} & \text{(Model A)} \\ -(1 - \delta_{kxi}) \nabla \cdot (p \bar{I}) + \nabla \cdot (\epsilon_k \bar{\tau}_{kv}) - \delta_{kxi} \nabla \cdot \bar{\tau}_{kc} & \text{(Model B)} \end{cases} \quad (3)$$

The kronecker delta function  $\delta_{kxi}$  is given by:

$$\delta_{kxi} = 1, \text{ if } k = s_i; \quad \delta_{kxi} = 0, \text{ if } k \neq s_i; \quad (4)$$

where  $k = s_i$  is a solids phase

The FLUFIX code is written in a modular form and has been demonstrated to be adaptable to a variety of problems. The conservation equations are solved in conservation law form using the IMF numerical technique [18].

The presence of the gradient of pressure in the fluid and solids phase momentum (Model A, Table I) results in an initial value problem that is ill-posed, as discussed in detail by Lyczkowski, et al. [19] This leads to a conditionally stable numerical solution. However, Model B (Table I) possesses real characteristics and is, therefore, well posed as an initial value problem.

In addition to increasing stability, the primary computational function of the Coulombic stress tensor for the solids,  $\sigma_{kc}$ , is to keep the bed from compacting below the defluidized packed bed state having a porosity of 0.38-0.4. Any model that accomplishes this is adequate. The Rietma and Mutsers model [21] used previously [7-9, 11-13] was found to be inadequate for cases involving obstacles and was subsequently modified to serve this purpose. The more subtle function of this term gained from computational experience is that it affects the instantaneous bed

interface and bubble shapes and timing. There is considerable disagreement as to the form of the solids stress term. We found no less than 15 forms summarized in Ref. 22. A systematic study of the sensitivity of the models for this term is planned.

The major empirical input in this cold bed is the fluid-particle drag coefficient,  $\beta$ . It is obtained from standard correlations [11-12].

## COMPUTATIONAL RESULTS AND COMPARISON WITH DATA

A model of fluidization in a two-dimensional rectangular bed with a central jet and a rectangular obstacle was set-up. The basic model is the same as published by Gidaspo and Ettehadleh [11] and is shown in Fig. 1. The computational region is 19.685 cm wide by 58.44 cm high. The cell sizes are  $\Delta x = 0.635$  cm,  $\Delta y = 4.87$  cm. Therefore, the number of computational cells is 31 in the x-direction and 12 in the y-direction for a total of 372. The number in parentheses refer to key cell numbers (I,J). Symmetry is assumed about the central jet so the actual bed width is 39.37 cm. The simulation was done before the experiment was performed. Previous modeling work without an obstacle [7] assumed symmetry and agreement with data was good. The jet half-width is 0.635 cm (one cell). The jet velocity is 578 cm/s and the secondary air velocity of 26 cm/s which is the minimum fluidization velocity. The particle diameter is 503  $\mu\text{m}$  and the density is 2.44  $\text{g/cm}^3$ . The obstacle, placed two nodes above the jet, is two nodes wide by two nodes high (1.27 cm wide and 9.74 cm high). Since the initial bed height is 29.22 cm (6 cells high), the obstacle lies completely within it.

The boundary conditions are as follows. At the inlet (J=2), the mass flux of gas is set equal to minimum fluidization conditions. The pressures in the dummy cells at the top (J=14) are set equal to atmospheric (1.013 x 10<sup>5</sup> Pa) and  $V_s = 0$ , that is a wire mesh is simulated to prevent solids carryover. The pressures in the bottom row of dummy cells are set equal to atmospheric pressure plus 1.2 times the total bed weight (1.0549 x 10<sup>5</sup> Pa). On all solid surfaces, no-slip boundary conditions are used, that is, normal and tangential velocities for each phase are set equal to zero. Free slip boundary conditions are used along the line of symmetry. Initially, the mass flux of gas in the bed is at minimum fluidization and the solids velocity is zero. The initial pressure distribution corresponds to the hydrostatic bed weight. At time 0+, the gas flow through the jet is increased to 578 cm/s.

Model A and B were used and overall both models compare well with experimental data as shown in Fig. 2. Sensitivity studies were also performed by using smaller mesh sizes and by varying the solids viscosity [23]. Typical results are shown in Fig. 3. A solids viscosity,  $\mu_s$ , of 1.0 Pa•s was used with model B and showed that the porosity oscillations were damped. Consequently, a solids viscosity of 0.1 Pa•s was used in all subsequent calculations. Such a value is in the range of experimentally measured viscosity in solids-gas fluidized beds [24]. Typical experimental porosity fluctuations recorded by means of a gamma ray densitometer are shown in Fig. 4. Spectral analysis of these data shows a major frequency of about 8 Hz, which is reasonably well predicted by model B (Fig. 3).

## CONCLUSIONS

Transient and time-averaged porosity distributions in a two-dimensional fluidized bed with an immersed obstacle were experimentally measured using a gamma-ray densitometer. Spectral analysis of these experimental data revealed the existence of characteristic bed frequencies, especially in the neighborhood of solids surfaces. Predicted time-averaged porosity distributions and characteristic frequencies of void fractions were found to be in good agreement with experimental data. This study further extends the validation of the two-phase flow hydrodynamic model, used in earlier study [25] to compare experimental and predicted bubble sizes.

## REFERENCES

1. LaNauze, R.D., "Fundamentals of Coal Combustion in Fluidized Beds," Chem. Eng. Res. Des., 63, pp. 3-33, (1985).
2. Muroyama, K. and L.S. Fan, "Fundamentals of Gas-Liquid-Solid Fluidization," AIChE J. 31, (1), pp. 1-34, (1985).

3. Lin, J.S., M.M. Chen and B.T. Chao, "A Novel Radioactive Particle Tracking Facility for Measurement of Solids Motion in Fluidized Beds," *AIChE J.* 31, (3), pp. 465-473, (1985).
4. Podolski, W.F., "Fluidized-Bed Combustion," in *The Science and Technology of Coal and Coal Utilization*, B. Cooper and W. Ellingson, eds., Plenum Press, New York, (1984).
5. Smoot, L., "Modeling of Coal-Combustion," in *The Science and Technology of Coal and Coal Utilization*, B. Cooper and W. Ellingson, eds., Plenum Press, New York, (1984).
6. Davidson, J.F., "Symposium on Fluidization-Discussion," *Trans. Inst. Chem. Engrs.*, 39, pp. 230-232, (1961).
7. Gidaspow, D., "Hydrodynamics of Fluidization and Heat Transfer: Supercomputer Modeling," 1984 D.Q. Kern Award Lecture presented at the 23rd National Heat Transfer Conference, Denver, CO (Aug. 5, 1985), *App. Mech. Rev.*, Vol. 39, No. 1, PP. 1-23, (Jan. 1986).
8. Gidaspow, D., B. Ettehadieh and R.W. Lyczkowski, "Computer Modeling of Fluidization of Sand in a Two-Dimensional Bed with a Jet," paper presented at AIChE 74th Annual Meeting, (Nov. 8-12, 1981).
9. Gidaspow, D., B. Ettehadieh, C.L. Lin and R.W. Lyczkowski, "Theoretical and Experimental Hydrodynamic of a Jet in a Fluidized Bed of Particles," *Proc. Intl. Symp. on Powder Technology*, 1981, Soc. of Powder Technology, Kyoto, Japan, pp. 672-681, (1982).
10. Gidaspow, D., C.L. Lin and Y.C. Seo, "Fluidization in Two-Dimensional Beds with a Jet. 1. Experimental Porosity Distributions," *I&EC Fund*, 22, pp. 187-193, (1983).
11. Gidaspow, D. and B. Ettehadieh, "Fluidization in Two-Dimensional Beds with a Jet. 2. Hydrodynamic Modeling," *I&EC Fund*, 22, pp. 193-201, (1983).
12. Ettehadieh, B., D. Gidaspow and R.W. Lyczkowski, "Hydrodynamics of Fluidization in a Demicircular Bed with a Jet," *AIChE J.* 30, (4), pp. 529-536, (1984).
13. Gidaspow, D., Y.C. Seo and B. Ettehadieh, "Hydrodynamics of Fluidization: Experimental and Theoretical Bubble Sizes in a Two-Dimensional Bed with a Jet," *Chem. Eng. Comm.* 22, pp. 253-272, (1983).
14. Rowe, P.N. and H. Masson, "Interaction of Bubbles with Probes in Gas Fluidized Beds," *Trans. Inst. Chem. Engrs.*, 59, pp. 176-185, (1981).
15. Rowe, P.N. and D.J. Everett, "Fluidized Bed Bubble Viewed by X-Rays, Part I - Experimental Details and the Interaction of Bubbles with Solid Surfaces," *Trans. Inst. Chem. Engrs.*, 50, pp. 42-48, (1972).
16. Fakhimi, S., and D. Harrison, "The Void Fraction Near a Horizontal Tube Immersed in a Fluidized Bed," *Trans. Inst. Chem. Engrs.* 58, pp. 125-131, (1980).
17. Rivard, W.C. and M.D. Torrey, "K-FIX: A Computer Program for Transient, Two-Dimensional, Two-Fluid Flow," Los Alamos Scientific Laboratory Report, LA-NUREG-6623, (Apr. 1977).
18. Rivard, W.C. and M.D. Torrey, "K-FIX: A Computer Program for Transient Two-Fluid Flow THREED: An Extension of the K-FIX Code for Three-Dimensional Calculations," Los Alamos Scientific Laboratory Report, LA-NUREG-6623, Suppl. II, (Jan. 1979).
19. Lyczkowski, R.W., D. Gidaspow, C.W. Solbrig and E.C. Hughes, "Characteristics and Stability Analyses of Transient One-Dimensional Two-Phase Flow Equations and Their Finite Difference Approximations," *Nuclear Science and Engineering*, (66), pp. 378-396, (1978).
20. Lyczkowski, R.W., "Transient Propagation Behavior of Two-Phase Flow Equations, in *Heat Transfer: Research and Application*," J.C. Chen, ed., *AIChE Symp. Series 75(174):165-174*, American Institute of Chemical Engineers, New York, (1978).
21. Rietma K. and S.M.P. Muters, "The Effect of Interparticle Forces on Expansion of a Homogeneous Gas-Fluidized Bed," in *Proceedings of International Symposium on Fluidization*, Toulouse, France, pp. 32-33, (1973).
22. Fayed, M.E. and L. Otten, "Handbook of Powder Science and Technology, p. 143, Van Nostrand Rheinhold Company, New York, (1984).
23. Bouillard, J.X., R.W. Lyczkowski, S. Folga, D. Gidaspow and G.F. Berry, "Hydrodynamics of Heat Exchanger Tubes in Fluidized Bed Combustors," Accepted for publication in *Canadian Journal of Chemical Engineering*, (Jan. 1988).
24. Grace, J.R., "Fluidized-Bed Hydrodynamics in *Handbook of Multiphase Systems*," G. Hetsoroni, ed., Chapter 8.1, pp. 8-5 to 8-64, McGraw-Hill, New York, (1982).
25. Lyczkowski, R.W., J.X. Bouillard and D. Gidaspow, "Computed and Experimental Motion Picture Determination of Bubble and Solids Motion in a Two-Dimensional Fluidized-Bed with a Jet and Immersed Obstacle," in *Proc. of the Eighth Intl. Heat Transfer Conference*, C.L. Tien, V.P. Carey and J.K. Farrell, eds., Vol. 5, pp. 2593-2598, Hemisphere Publ. Corp., Washington, D.C., (1986).

## NOMENCLATURE

|               |                                      |
|---------------|--------------------------------------|
| $\rightarrow$ |                                      |
| $g$           | Acceleration due to gravity, $m/s^2$ |
| $=$           |                                      |
| $I$           | Unit tensor                          |
| $n$           | Number of phases                     |
| $p$           | Pressure, Pa                         |
| $t$           | Time, s                              |
| $\rightarrow$ |                                      |
| $v_k$         | Velocity of phase k, m/s             |

### Greek Letters

|                |                                                                  |
|----------------|------------------------------------------------------------------|
| $=$            |                                                                  |
| $\beta_{ik}$   | Fluid-particle drag tensor, $kg/(m^3.s)$                         |
| $\delta_{ksj}$ | Kronecker delta function given by Eq. (4)                        |
| $\epsilon_k$   | Volume fraction of phase k                                       |
| $\rho_k$       | Density of phase k, $kg/m$                                       |
| $=$            |                                                                  |
| $\sigma_{ke}$  | Effective phase stress tensor of phase k, defined by Eq. (3), Pa |
| $=$            |                                                                  |
| $\tau_{kc}$    | coulombic stress tensor for solids ( $k = s_i$ ), Pa             |
| $=$            |                                                                  |
| $\tau_{kv}$    | Microscopic viscous stress tensor of phase k, Pa                 |

### Superscripts

|               |                           |
|---------------|---------------------------|
| $\rightarrow$ | Denotes a vector quantity |
| $=$           | Denotes a tensor quantity |

## DISCLAIMER

This report was prepared as an account of work sponsored by an agency of the United States Government. Neither the United States Government nor any agency thereof, nor any of their employees, makes any warranty, express or implied, or assumes any legal liability or responsibility for the accuracy, completeness, or usefulness of any information, apparatus, product, or process disclosed, or represents that its use would not infringe privately owned rights. Reference herein to any specific commercial product, process, or service by trade name, trademark, manufacturer, or otherwise does not necessarily constitute or imply its endorsement, recommendation, or favoring by the United States Government or any agency thereof. The views and opinions of authors expressed herein do not necessarily state or reflect those of the United States Government or any agency thereof.

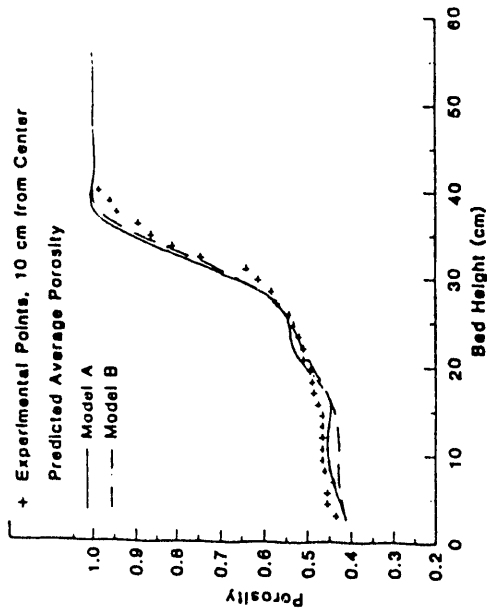


FIGURE 2 Experimental and Theoretical Time-Averaged Vertical Profiles for Two Hydrodynamic Models.

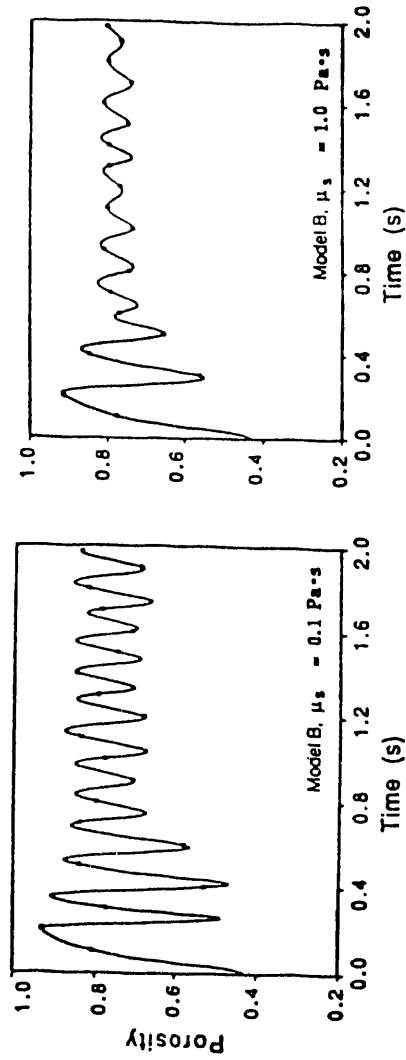


FIGURE 3 Predicted Instantaneous Porosity as a Function of Solids Viscosity.

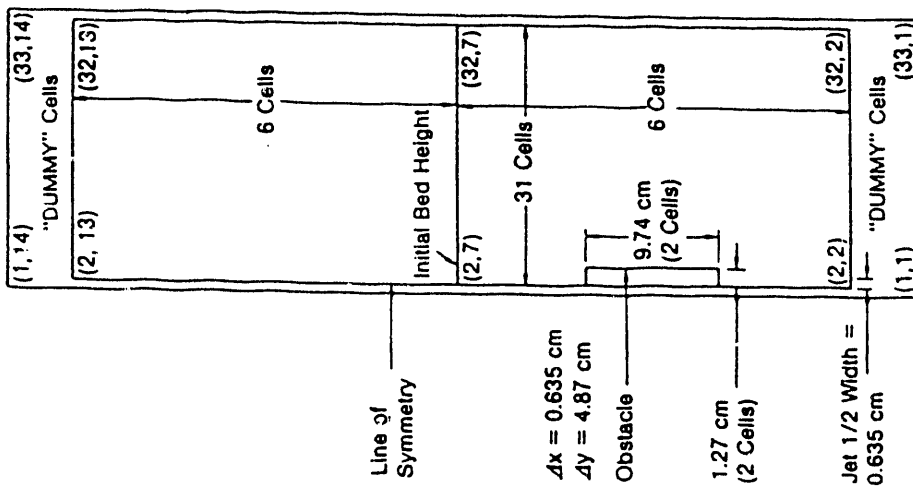


FIGURE 1 Computational Mesh for Coarse Mesh Showing Obstacle Location.

LOCATION:

X = 0.0 cm

Y = 1.27 cm

SAMPLING FREQUENCY = 50 Hz

BUBBLING FREQUENCY = 7.5 Hz

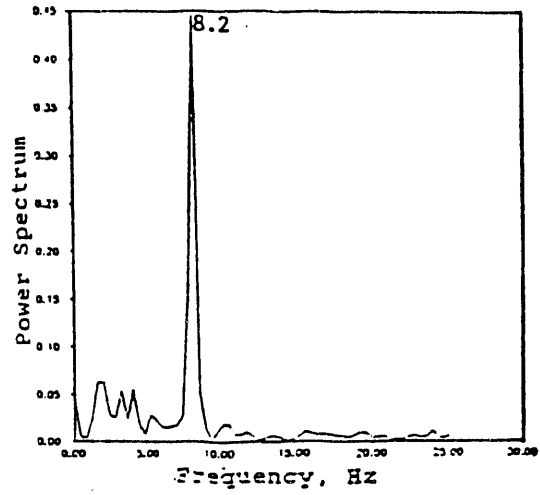
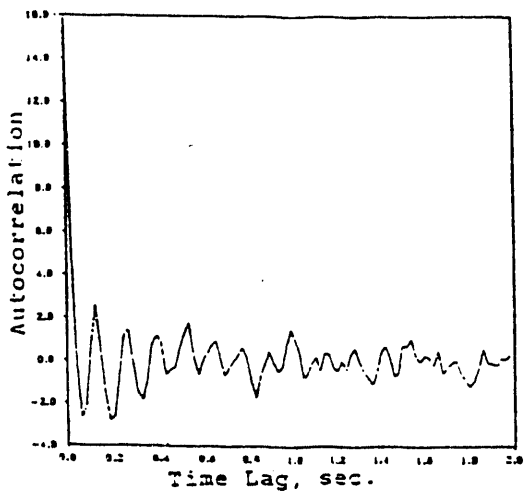
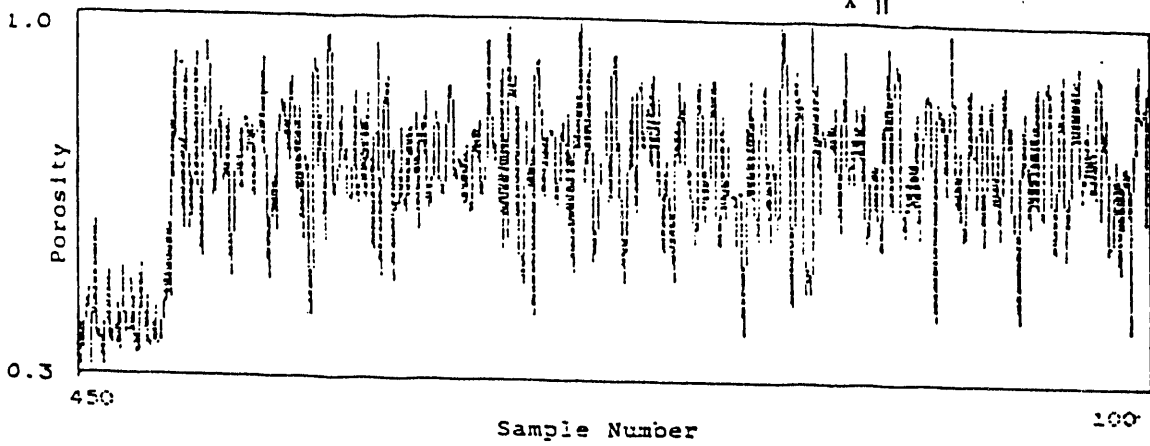
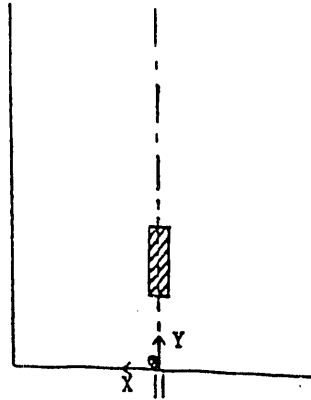


FIGURE 4 Typical Experimental Transient Porosity History with its Power Spectral Analysis.

**END**

**DATE  
FILMED**

**2 / 2 / 93**

